Geologica Acta, Vol.7, Nos 1-2, March-June 2009, 281-296
DOI: 10.1344/105.000000282
Available online at www.geologica-acta.com

geologica acta

Integrated calcareous nannofossil biostratigraphy and magnetostratigraphy from the uppermost marine Eocene deposits of the southeastern Pyrenean foreland basin: evidences for marine Priabonian deposition

ANTONIO CASCELLA [1] **and JAUME DINARÈS-TURELL** [2]

[1] **Istituto Nazionale di Geofisica e Vulcanologia (INGV)**
Via della Faggiola, 32, I-56126 Pisa, Italy. E-mail: cascella@pi.ingv.it

[2] **Istituto Nazionale di Geofisica e Vulcanologia (INGV)**
Via di Vigna Murata, 605, I-00143 Rome, Italy. E-mail: dinares@ingv.it

ABSTRACT

An integrated magneto-biostratigraphic study, based on calcareous nannofossils, was carried out on the Eocene uppermost marine deposits of the southeastern Pyrenean foreland basin. The study was performed along six sections of the upper portion of Igualada Formation, cropping out in the Vic area. Common late Middle/Upper Eocene nannofossil assemblages allow recognizing, within a normal magnetozone or immediately below, the FO of *Istmolithus recurvus*, which identifies the base of NP19 Zone, in the Priabonian. This event occurs within C16n.2n magnetozone in several oceanic and Mediterranean sections, which allows the correlation of the normal magnetozone in the Vic area to chron C16n.2n. This challenges previous magnetostratigraphic interpretations in the Vic area that correlated the uppermost marine sediments to chron C17n. The estimated age for the FO of *I. recurvus* is 36 Ma and collectively with the magnetostratigraphic data indicates that the uppermost marine sediments in the basin are of Priabonian age. The new results indicate that the entire chronology of the marine strata needs reassessment. The thickness of chron C16n.2n varies from 45 m in the Collsuspina area (southern sector) to about 270-290 m in the Sant Bartomeu del Grau area (northern sector), which is indicative of a marked asymmetry in the basin deposition.

KEYWORDS | **Late Eocene. Magnetostratigraphy. Biostratigraphy. Calcareous Nannofossils. Pyrenean basin.**

INTRODUCTION

Basin analyses require precise dating, but poor outcrops, stratigraphic discontinuity and facies changes often hamper this. In the southeastern Pyrenean foreland basin (Fig. 1), the occurrence over short distances of shallow-water facies, mainly containing benthic microfossils, and deep-water facies, characterized by planktonic microfossils, generally made difficult cross basin correlations, for the difficulty to correlate biostratigraphies based on

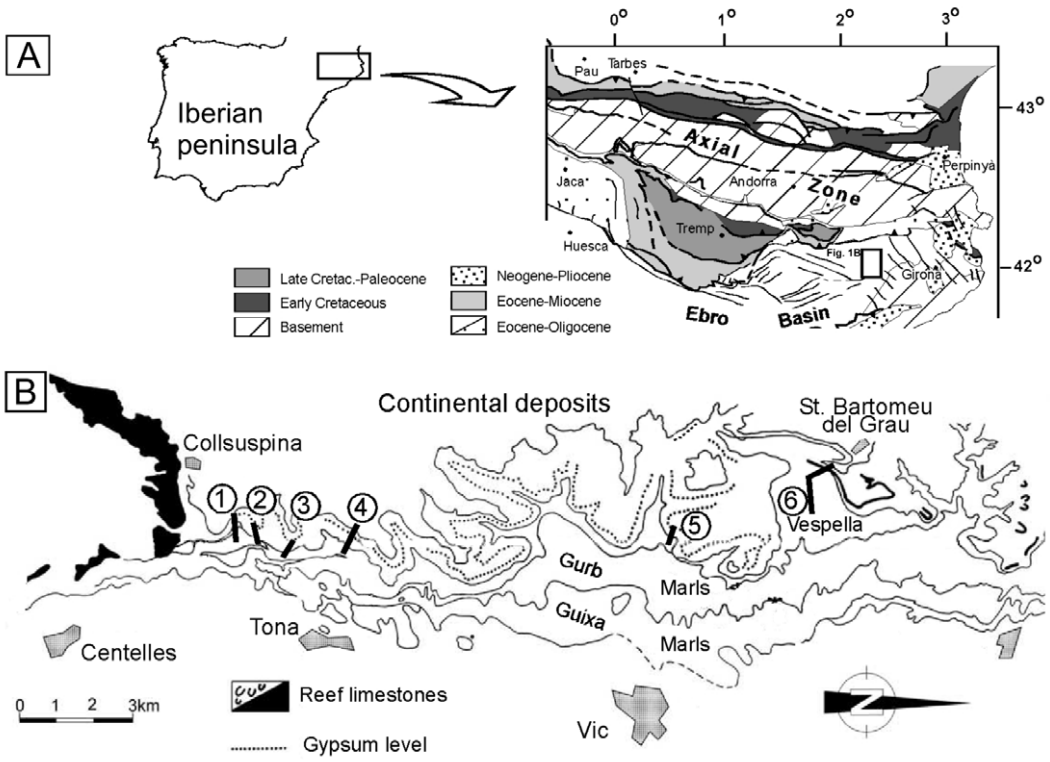

FIGURE 1 **A) Geological map with location of the Vic area (squared) in the northeastern part of the Ebro basin. B) Geological map with lithostratigraphic units of the studied sector in the Vic area (modified from Pisera and Busquets, 2002). Numbers refer to the studied sections: 1) Collsuspina1; 2) Collsuspina2; 3) Tona; 4) Múnter; 5) Gurb; 6) Sant Bartomeu del Grau.**

planktonic microfossils with those based on larger foraminifers (Luterbacher, 1998; Taberner et al., 1999). During the two last decades, calcareous nannofossils showed to be a powerful tool in terms of regional and worldwide stratigraphic correlations. Some distinctive characters make these microfossils useful in correlating shallow and deep sectors of a basin, enabling the link of biostratigraphic data from different microfossil groups (benthic and planktonic) to other stratigraphic data (magnetostratigraphy). They are usually abundant, occur also in shallow marine sediments where planktonic foraminifera are very rare or absent, the analyses of the assemblages require a small amount of sediment that allows to sample also thin shale layers in sand dominated lithostratigraphic sections.

Calcareous nannofossils were poorly investigated in the Pyrenean foreland basin (Anadón et al., 1983; Canudo et al., 1988) and never in the Vic area. Previous biostratigraphy was focused mainly on the analyses of the rich larger foraminifer assemblages, which provided the data used for the compilation of part of the Paleocene-Eocene Shallow Benthic Zones of Serra-Kiel et al. (1998). However, the record of diagnostic upper Middle to Upper Eocene calcareous nannofossil assemblages, from some pilot-samples, including carbonate platform lithofacies, of the Vic marine succession, encouraged us to undertake an extensive investigation of these planktonic microfossils. In this paper we report on new calcareous nannofossil and magnetostratgraphic data for the uppermost marine sequence, along several sections from the central and northern parts of the basin in the Vic area, suggesting the revision of previous biostratigraphic and chronostratigraphic assignments.

GEOLOGICAL SETTING

The Paleogene marine sediments of the southeastern Pyrenean foreland basin (Ebro basin) constitute four tectostratigraphic sequences of Ypresian through Bartonian/early Priabonian (?) age (Serra-Kiel et al., 2003b). The sedimentation starts with a transgressive system composed of the shallow-marine Alveolina limestone of the Cadí Formation (Fm) (Ypresian) and is normally capped by the evaporite Cardona Fm (lower Priabonian) followed by Oligocene continental deposits. At the easternmost side of the basin, Vic area (Fig. 1), the marine succession, considered to be middle Lutetian to late Bartonian in age, consists of the following formations from the bottom

(Fig. 2): Banyoles Marls, Tavertet Limestones, Coll de Malla Marls, Folgueroles Sandstones, Igualada Marls (subdivided into Manlleu Marl, La Guixa and Gurb Marl, Vespella Marl members) and the Terminal Complex (consisting of sandstones, anoxic marls, stromatholits and gypsum). Particularly the marls of the Igualada Fm are locally punctuated by carbonate facies and reef of the La Tossa Fm (to the south) and the St. Martí Xic Fm (to the north). At the easternmost side of the basin (Vic area) the marine succession, which is sandwiched between Paleocene and Oligocene continental deposits is traditionally considered to be middle to upper Eocene in age (based mostly on larger foraminifera biostratigraphy) (Serra-Kiel et al., 1997 and references therein). In that framework, the basal marine strata have been dated as middle Lutetian age (east of Vic) to Bartonian age in the southern sector of the basin, emphasizing a strong diachroneity of the base of the marine deposits. This interpretation was controversially challenged by Taberner et al. (1999) on the basis of magnetostratigraphic data and numerical age constraints ($^{40}Ar/^{39}Ar$ dating on glauconite crystals) from the southern sector of the basin suggesting that marine deposition also started there in the Lutetian, some 5 Myr earlier than previously inferred (see also Serra-Kiel et al., 2003a, b, c; Taberner et al., 2003). Instead, Taberner et al. (1999) propose that a marked basin asymmetry is observed later in its evolution.

PREVIOUS CHRONOSTRATIGRAPHIC STUDIES

The studied sediments interested the geologists since the middle of the nineteenth century, being the object of numerous stratigraphic, sedimentologic, magnetostratigraphic and biostratigraphic studies (see Reguant, 1967; Ferrer, 1971; Burbank et al., 1992; Taberner et al., 1999; Romero and Caus, 2000; Serra-Kiel et al., 2003a and b, and references therein).

The chronostratigraphic assignments were based mostly on larger foraminifer biostratigraphy, discontinuous planktonic foraminifera data from neighbouring areas, combined with magnetostratigraphic information (Serra-Kiel et al., 2003a and b), or on magnetostratigraphy and numerical age dating on glauconite (Taberner et al., 1999). Some disagreement exists about the beginning and the end of the marine sedimentation in this sector of the basin. Particularly, the chronostratigraphic proposal of Taberner et al. (1999) is in contradiction with earlier biostratigraphic studies as pointed before, implying a shift of some 5 My in the age of the earliest marine sediments (Serra-Kiel et al., 2003c; Taberner et al., 2003).

As far as the end of the marine sedimentation is concerned, it has been controversially considered late Bartonian or early Priabonian in age. Ferrer (1971) assigned the

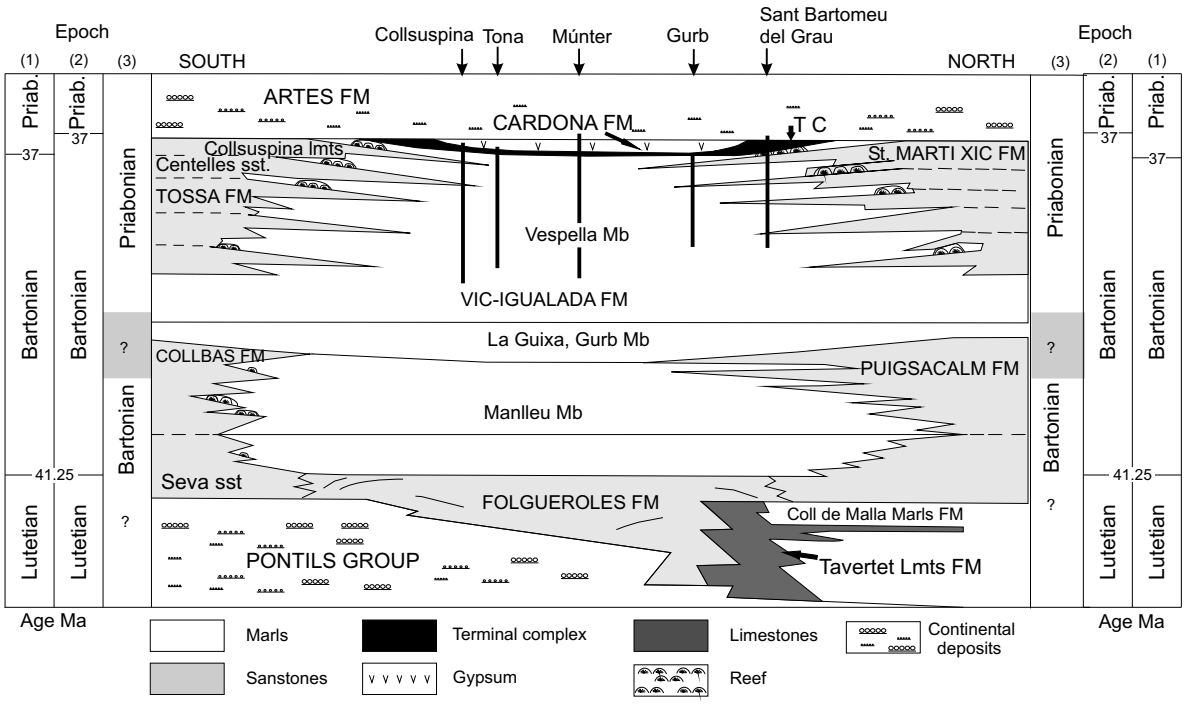

FIGURE 2 | **Chronostratigraphic diagram from the Vic sector of the southern Pyrenean foreland basin (modified from Pisera and Busquets, 2002). Chronological schemes are from 1) Taberner et al. (1999) and from 2) Burbank et al. (1992). 3) In this study we propose a Bartonian/Priabonian boundary in a lower position within the Vespella Marl member or even lower. The labelled arrows on the top of the diagram indicate the relative position of the studied sections shown as vertical bars.**

upper portion of the Igualada Fm in its type area to the early Priabonian on the basis of planktic foraminifers from the Zone P15. Serra-Kiel et al. (2003b) dated these sediments to the Shallow Benthic Zone (SBZ18), and correlated them to magnetochron 17 following the magnetostratigraphic section in the Vic area of Burbank et al. (1992). Consequently, the upper Eocene is not represented in this area by marine sediments as reflected by the absence of larger foraminifera from the SBZ 19 Zone (Romero and Caus, 2000). Taberner et al. (1999) stressed a diachrony of the top of the marine deposits on the basis of a northward increase in the thickness of a normal chron correlated to C17n.1n, in conjunction to the presence of younger additional magnetozones within marine strata at the top of the marine interval in the northern sector (Sant Bartomeu del Grau quarry section). In addition, Canudo et al. (1988) reported Priabonian calcareous nannofossils (Zone NP18) and larger foraminifers (Zone *Nummulites fabiani*) from the equivalent Arguís Fm, in the prepyrenean zone of Aragon.

The identification of the boundary between the Bartonian and the Priabonian, i.e. the Middle Eocene/Late Eocene boundary, is difficult for the occurrence of a major hiatus at the base of Priabonian stratotype (Veneto, Italy). Therefore, the base of the Priabonian is discussed and remains unsolved until a reference section with a suitable GSSP (Global Stratotype Section and Point) will be found (Verducci and Nocchi 2004). For these purpose, Rio et al. (2006) have proposed the Alano di Piave section (Venetian Southern Alps, NE Italy) as a potential GSSP of the Priabonian Stage although the studies are still undergoing. Up till now, this boundary can be traced either at the base of Zone *Nummulites fabiani* s.s. or at the base of underlying Zone *N. variolatus/incrassatus* (Papazzoni and Sirotti 1995). In Serra-Kiel et al. (1998), the boundary between the macroforaminiferal biozones SBZ18 and SBZ19, defined on the basis of the First Occurrence (FO) of *Nummulites fabiani*, is equated with the Bartonian/Priabonian boundary and considered to fall in the middle of the planktonic Zone P15 of Berggren et al. (1995), near the top of chron C17n. In terms of calcareous nannofossils, Berggren et al. (1995) traced it in correspondence with the NP17/NP18 nannofossil zone of Martini (1971), defined by the FO of *Chiasmolithus oamaruensis*, within Zone P15 of Blow (1969).Varol (1998) considered the Last Occurrence (LO) of *C. grandis*, just below the first occurrence of *C. oamaruensis*, to approximate the boundary between the Bartonian and the Priabonian stages.

SAMPLING AND METHODS

The sediments investigated belong to the uppermost portion of Igualada Fm (Ferrer, 1971), just below a transitional unit preceding the gypsum deposits that are linked to the Cardona salt Formation by Riba (1967, 1975). The lithostratigraphic studied interval consists of marine deep outer shelf marls (prodelta marls), which display a conspicuous lithologic cyclicity of relatively carbonatic rich and carbonate poor layers. These marls and the transitional unit above up to the evaporitic unit or to the continental deposits (Artés Fm), were sampled along the Collsuspina, Tona, Múnter, Gurb and Sant Bartomeu del Grau localities, comprising a total of 6 subsections (Figs. 2, 3 and 4). These sections represent a transect of 16 km that extents from the southern margin (Collsuspina) to the northern margin of the basin (Sant Bartomeu del Grau). At the Múnter_1 and Sant Bartomeu del Grau subsections the lowermost continental red sandstones from the Artés Fm were also sampled.

Paleomagnetic samples were collected in the field as oriented hand-samples (only occasionally a drill corer was used) and subsequently prepared in the laboratory for standard measurements. Sampling spacing is variable (about every 2-5 m normally) and takes in consideration previous magnetostratigraphies in the basin (Taberner et al., 1999). Natural remanent magnetization (NRM) and remanence through all demagnetization stages were measured using a 2G-Enterprises high-resolution (45 mm diameter) pass-through cryogenic magnetometer equipped with DC-squids and operating in a shielded room at the Istituto Nazionale di Geofisica e Vulcanologia in Rome, Italy. Alternating field -(AF) demagnetisation was performed with three orthogonal coils installed inline with the cryogenic magnetometer. Orthogonal vector demagnetisation plots (Zijderveld, 1967) were used to represent demagnetisation data and a least-squares line-fitting procedure (Kirschvink, 1980) was used to determine the magnetisation components. Normally one specimen per stratigraphic level (occasionally two) was routinely subjected to stepwise alternating field (AF) demagnetisation, up to 100 mT, including 14 steps with intervals of 5, 10 and 20 mT. A single heating step of 150ºC was applied before AF demagnetisation in most cases. A total of 188 specimens were fully demagnetised for the present study.

The analysis of calcareous nannofossils was carried out on a total of 121 samples, prepared as smear slides using standard procedure (Bown, 1998). The taxa identifications were performed by a polarized light microscope Leica DMLP 100 at 1250x magnification. The assemblages were qualitatively and semi-quantitatively characterized in terms of preservation and abundance (Tables 1-5). Calcareous nannofossil total abundance was estimated as number of specimens for field of view. The abundance of each species was detected by counting 300 nannofossils. Moreover, at least two additional traverses of each

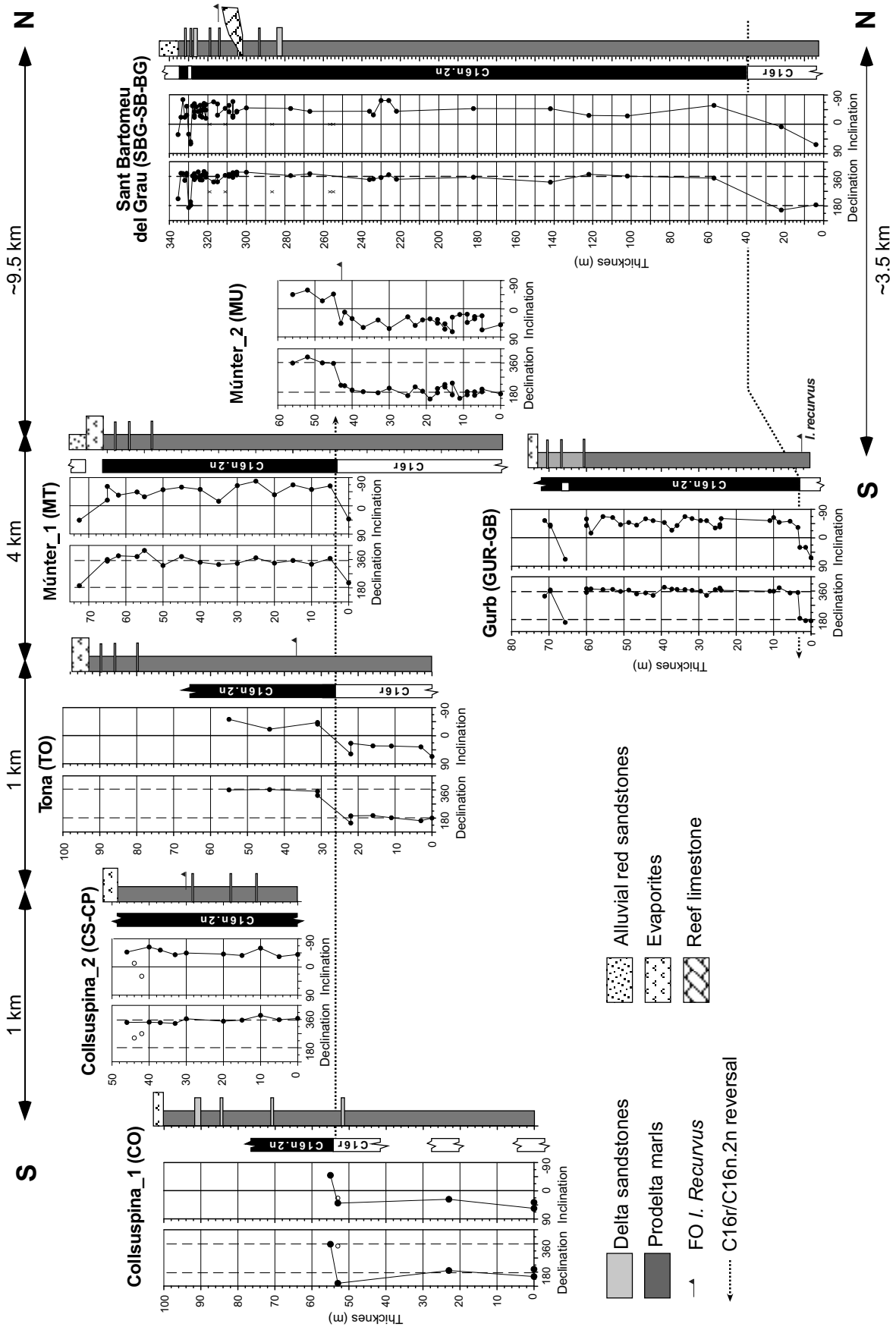

FIGURE 3 | **Simplified lithologic logs for the different studied sections with ChRM declination and inclination plots. Open circles denote unreliable data and crosses mark the position of samples that have provided no data. The identified chrons and the FOs of *I. recurvus* are indicated.**

slide were scanned in order to recognize the presence of very rare species. We refer to Perch-Nielsen (1985), Catanzariti et al. (1997), Bown (1998) and Aubry (1999) for the description of the nannofossils recorded.

RESULTS

Calcareous nannofossil biostratigraphy

The standard scheme of Martini (1971) has been adopted for this study. Concerning the Priabonian Zones NP19 and NP20, we adopted the combined Zone NP19 - NP20 because the boundary between the aforesaid biozones, marked by the FO of *Sphenolithus pseudoradians*, has been shown to be unreliable being this species already observed in Middle Eocene deposits (Aubry, 1992, Luciani et al., 2002). The Martini's biozones have been correlated to the zonal schemes of Okada and Bukry (1980) and Catanzariti et al. (1997). Moreover, the calcareous nannofossil biozonation has been correlated to the planktonic foraminiferal zones of Berggren et al. (1995) and to the benthonic foraminiferal zones of Serra-Kiel et al. (1998) and integrated to the geochronological time-scale of Berggren et al. (1995) (Fig. 5).

The samples analyzed contain few to common and moderately preserved calcareous nannofossils (Tables 1-5). Most significant taxa are illustrated in Fig. 6. The assemblages are specially characterized by *Cyclicargolithus floridanus*, *Coccolithus pelagicus*, *C. eopelagicus*, *Lanternithus minutus* (Fig. 6A), *Cribrocentrum reticulatum* (Fig. 6B), *Dictyococcites bisectus* (Fig. 6C) and *Zigrablithus bijugatus*. The taxa *C. formosus*, *Reticulofenestra umbilica* (Fig. 6D), *Sphenolithus predistentus* and *S.* spp, *Discoaster saipanensis* (Fig. 6E), *D. barbadiensis*, *Helicosphaera compacta*, *H. bramlettei* and *H. euphratis*, are less frequent. *Chiasmolithus* genus consists of rare broken specimens, among them *C. oamaruensis* (Fig. 6F) was recognized. *Isthmolithus recurvus* (Figs. 6G and K) is rare and discontinuous. It is worth noting the occurrence of specimens of *Cribrocentrum* sp. (Fig. 6L), referable to *Cribrocentrum* sp1 of Fornaciari et al. (2006) (Catanzariti, "pers. comm."), not distinguished in the distribution Tables 1-5. Cretaceous and Paleogene reworked taxa occur as well.

The assemblages including *C. oamaruensis* and *I. recurvus* are of the Priabonian Zones NP18 and NP19-NP20 of Martini (1971), respectively. Zone NP18 is dubitatively also assigned to the other samples on the basis of

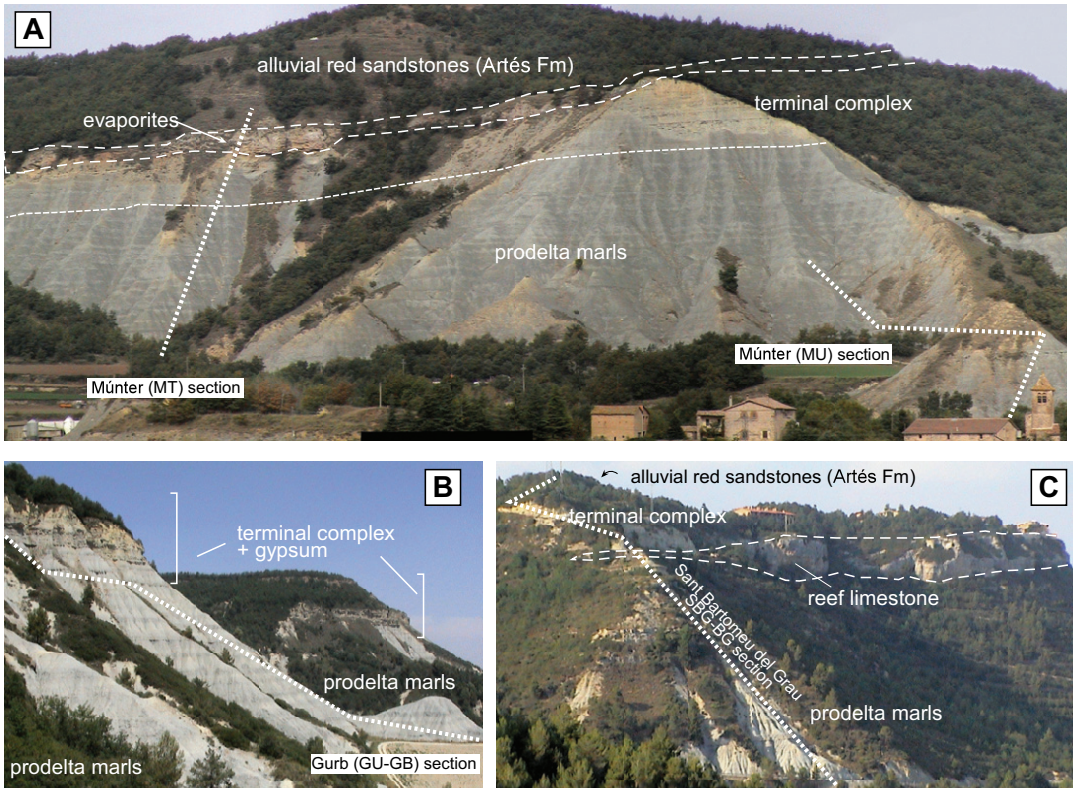

FIGURE 4 | **Field photographs of the uppermost marine sediments at three of the studied localities. A) Múnter, B) Gurb, and C) Sant Bartomeu del Grau.**

the absence of *C. grandis*, occurring in lower portions of the Vic succession (Cascella and Dinarès-Turell, unpublished data), and the occurrence of *Cribricentrum* sp. described from Upper Eocene sediments from the Northern Apennines and oceanic areas (Catanzariti et al., 1997, Fornaciari et al. 2006). Following the integrated chronostratigraphic scheme (Fig. 5), the investigated interval falls between the middle part of planktic foraminiferal Zone P15 and the upper part of Zone P16 of Berggren et al. (1995), and between the larger foraminiferal Zones SBZ19 and SBZ20 of Serra-Kiel et al. (1998).

Magnetostratigraphy

In general, the intensity of the NRM was moderate around 4 x 10^{-3} A/m for normally magnetized samples and it was lower for samples with a reverse characteristic remanent magnetisation (ChRM) due to overlap of a normal recent overprint. Two magnetisation components can be recognized in most samples upon demagnetisation, in addition to a viscous magnetisation removed below 5 mT or 150°C. Component L is unblocked usually below 20-25 mT and conforms to the present magnetic field (Fig. 7). Component H is unblocked above 25 mT, conforms the ChRM and has either normal or reverse polarity in bedding-corrected coordinates (Fig. 7). Most of the studied samples show high-quality demagnetization data and magnetic polarity can be established unambiguously. Due to the gentle dipping of the studied succession a fold-test cannot be performed. Mean declination and inclination for the ChRM component after bedding-correction is consistent with previous data from the basin (Taberner et al., 1999). Mean normal and reverse directions are practically antipodal (Fig. 8) and conform a positive class A reversal test (McFadden and McElhinny, 1990). Statistical parameters improve slightly upon tilt correction (Fig. 8). The declination and inclination of the ChRM components have been used to derive the local magnetostratigraphy (Fig. 3). Given the biostratigraphic constraints (see above) the normal chron below the evaporitic unit has to be correlated to chron C16n.2n with an age of 35.707 Ma and 36.276 Ma for its top and base respectively as estimated in the most recent timescale (Gradstein et al., 2004).

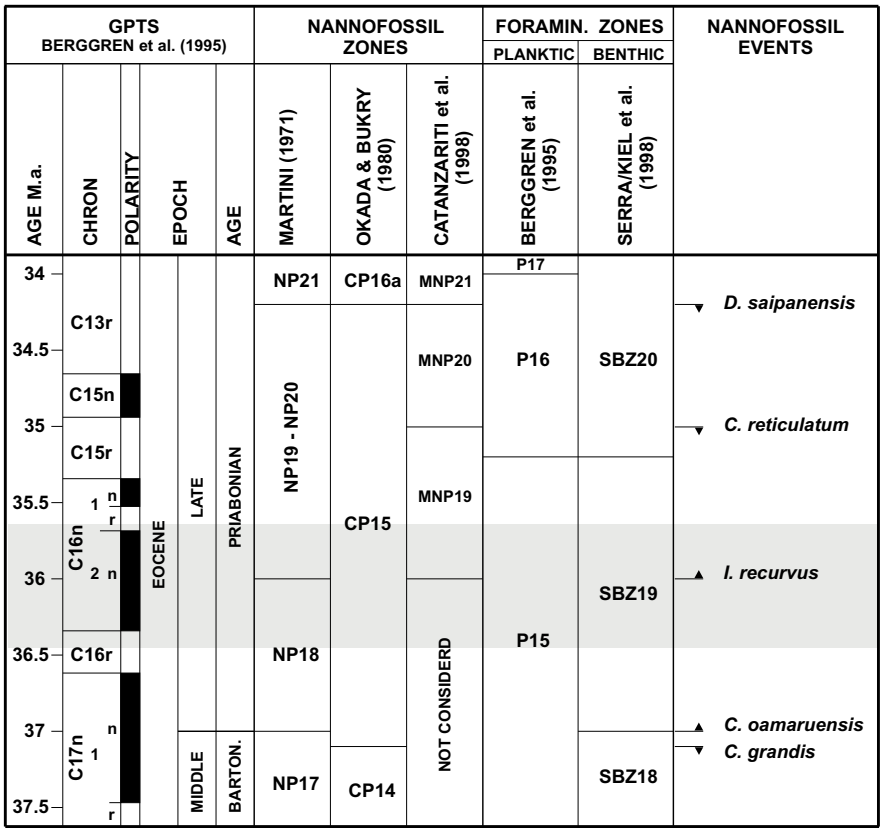

FIGURE 5 **Latest Middle to Late Eocene magneto-bio-cronostratigraphy. The calcareous nannofossil biozonations of Martini (1971), Okada and Bukry (1980), and Catanzariti et al. (1997), have been correlated with the planktonic foraminiferal zones of Berggren et al. (1995) and the benthonic foraminiferal zones of Serra-Kiel et al. (1998). Geochronological time-scale (GPTS) is from Berggren et al. (1995). The shaded box roughly indicates the time interval covered by the studied sections in this study.**

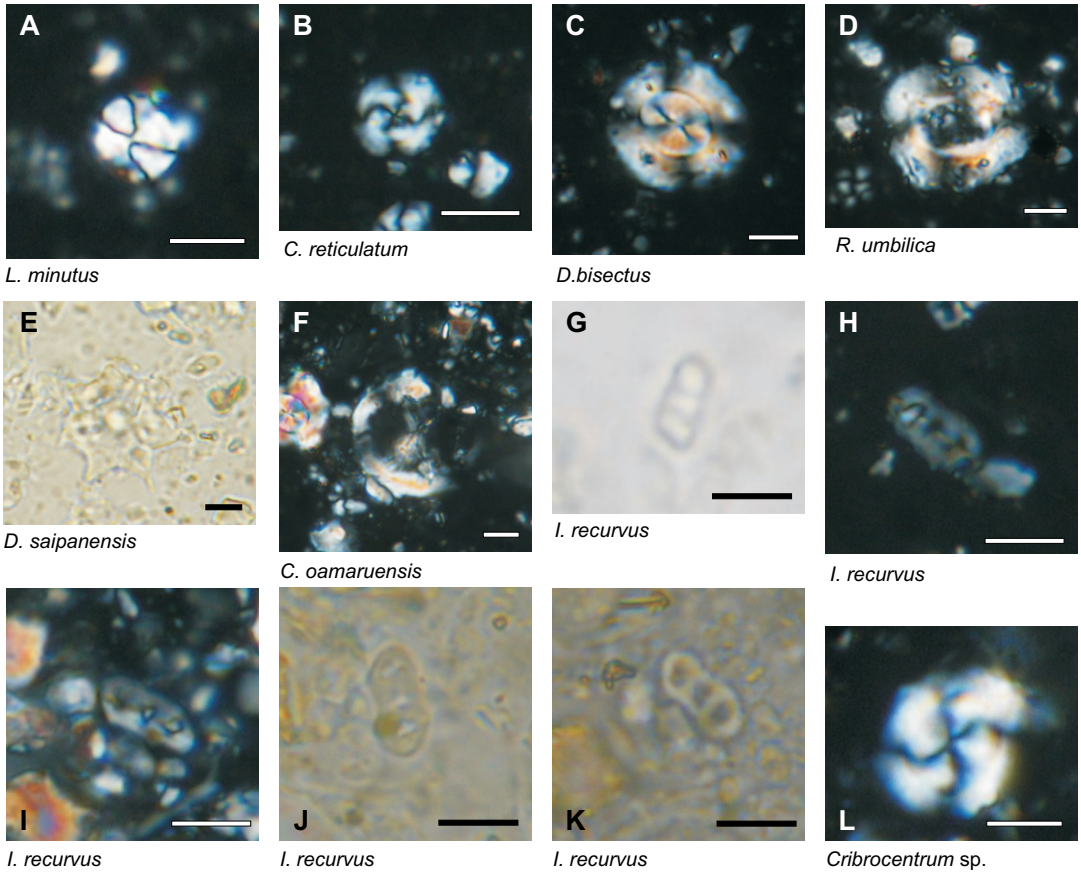

FIGURE 6 | **Light micrography: XP = cross-polarized light, PL = plain transmitted light. Scale bar = 5 µm. A) *Lanternithus minutus* Stradner, 1962; Gurb Section, sample GUR29; XP. B) *Cribrocentrum reticulatum* (Gartner and Smith, 1967) Perch-Nielsen, 1971; Gurb Section, sample GUR29; XP. C) *Dictyococcites bisectus* (Hay, Mohler and Wade, 1966) Bukry and Percival, 1971; Gurb Section, sample GUR33; XP. D) *Reticulofenestra umbilica* (Levin, 1965) Martini and Ritzkowski, 1968; Gurb Section, sample GUR33; XP. E) *Discoaster saipanensis* Bramlette and Riedel, 1954; Gurb Section, sample GUR2; PL. F) *Chiasmolithus oamaruensis* (Deflandre, 1954) Hay, Mohler, and Wade, 1966.; Gurb Section, sample GUR35; XP. G,H) *Isthmolithus recurvus* Deflandre in Deflandre and Fert, 1954; Gurb Section, sample GUR24; G) PL and H) XP. I, J, K) *Isthmolithus recurvus* Deflandre in Deflandre and Fert, 1954; Gurb Section, sample GUR38; I) XP and J,K) PL. L) *Cribrocentrun* sp.; Gurb Section, sample GUR39; XP.**

DISCUSSION

Coccolithophorids distribution is largely controlled by temperature, water mass conditions and trophic resources (Aubry, 1992; Persico and Villa, 2004). The identified assemblages in this study are characterized by low diversity, common temperate eutrophic species (such as *C. floridanus*, *C. reticulatum*, *L. minutus*) (Persico and Villa, 2004), common near shore indicators (*L. minutus* and *Z. bijugatus*) (Nocchi et al., 1988) and scarce warm oligotrophic species (*Sphenolithus* and *Discoaster*) (Aubry, 1992). Thus, the nannoflora reflect the marginal- sea character of the investigated sediments and the cooling that occurred during the Middle and Late Eocene.

The appearance of C. *oamaruensis* usually precedes the *I. recurvus* FO (Fig. 5). In the studied sediments, this sequence has been recorded only in the Múnter section (Table 3), throughout the other sections the two index species occur simultaneously (Tona and Gurb sections, Tables 2 and 4) or the sequence is reverse (S. Bartomeu del Grau section, Table. 5). Most likely this is due to the rarity and discontinuous presence of *C. oamaruensis*, in agreement with the generally scarce presence of *Chiasmolithus* genus in the Mediterranean Upper Eocene sediments (Nocchi et al., 1988; Catanzariti et al., 1997; Luciani et al., 2002).

The FO of *Istmolithus recurvus* occurs within C16n.2n magnetozone in several oceanic and Mediterranean sections and is calibrated at 35,9 and at 36 Ma (Berggren et al., 1995; Marino and Flores, 2002; Jovane et al., 2007). As far as our study, very rare and poor preserved specimens of *I. recurvus* first occur in the uppermost portion of the reversal magnetozone correlated to chron C16r. In the Tona, Múnter and Gurb sections the lowest occurrence of this

species is slightly older than the C16r/C16n.2n reversal boundary, whereas it appears in the lower part of chron C16n.2n in the Collsuspina section or even higher in C16n.2n in the Sant Bartomeu del Grau section (Fig. 3). So, our current dataset assigns the FO of *I. recurvus* close to the C16r/C16n.2n. These data suggest a heterochrony for this bioevent; but our lowest occurrence, consisting of very rare specimens, does not correspond with the more consistent appearance within chron C16n.2n, which likely represents the first regular and/or common occurrence of the species in the stratigraphic record. This latest event could be identified in the Gurb section from the sample Gur33, within normal chron C16n.2n.

The *I. recurvus* FO has been correlated with the Priabonian SBZ19 (Zone *N. fabianii* s.s.) (Luciani et al., 2002). The occurrence of this species, in the younger

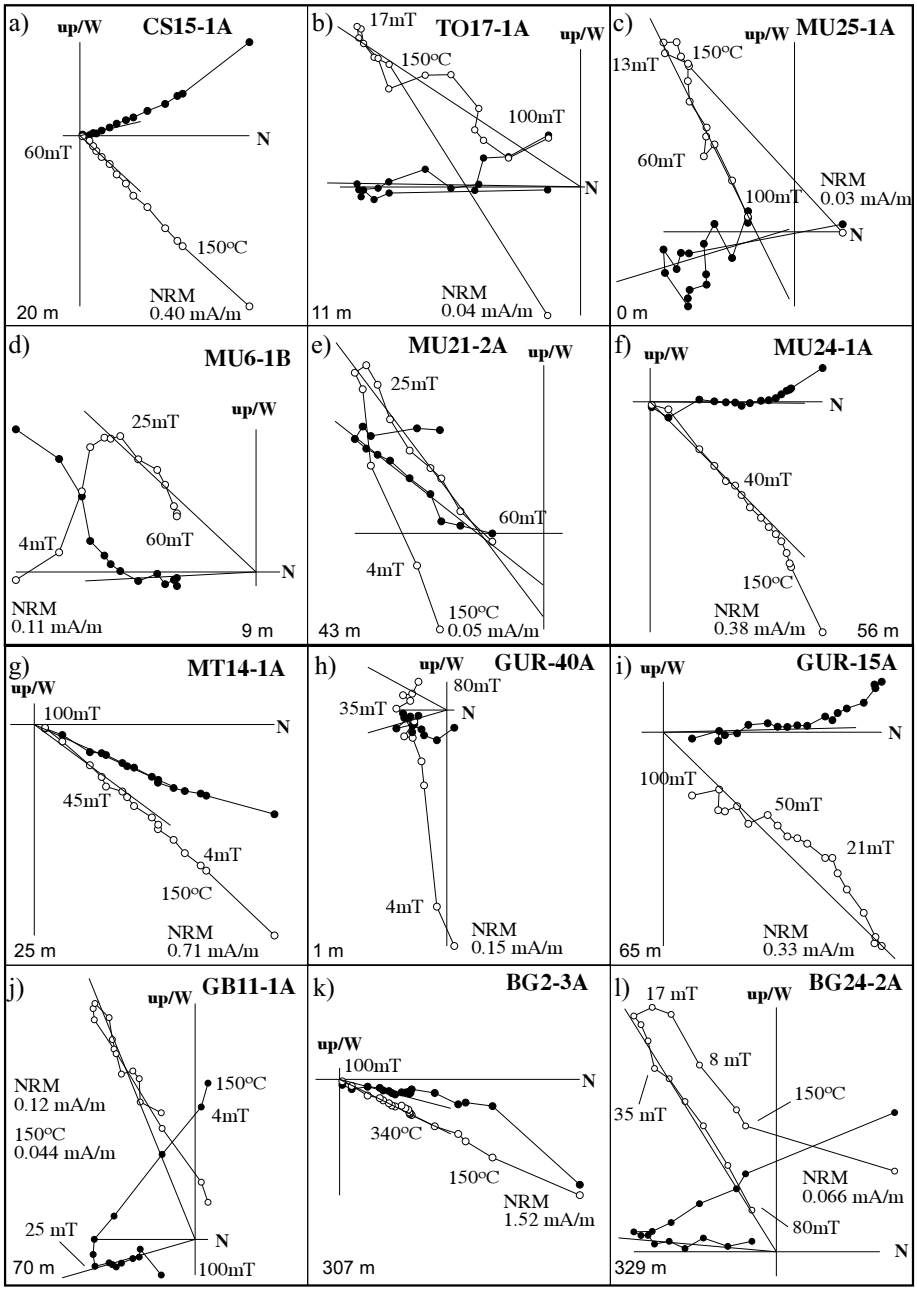

FIGURE 7 | **Bedding-corrected orthogonal plots of alternating field demagnetisation data from normal (a, f, g, i, k) and reverse (b, c, d, e, h, j, l) specimens from different sections. Solid (open) symbols represent projections onto the horizontal (vertical) plane. The fitted ChRM direction, the natural remanent magnetization (NRM) intensity, the stratigraphic level in meters, and some step treatments are indicated for each example.**

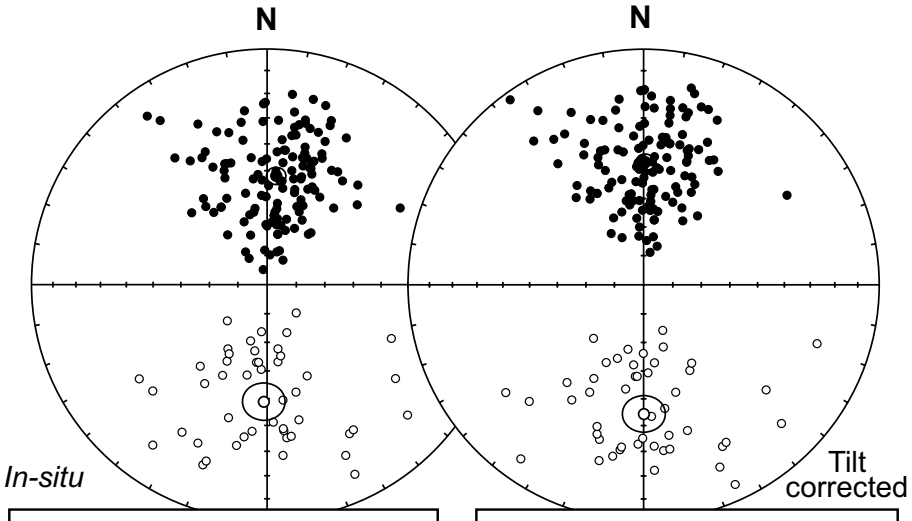

Sample	N	Dec.	Inc.	k	α_{95}
Normal	132	4.8	51.8	16.1	3.2
Reverse	47	181.6	-48.8	10.1	6.9

Sample	N	Dec.	Inc.	k	α_{95}
Normal	132	0.8	46.9	16.7	3.1
Reverse	47	179.9	-44.3	10.2	6.8

FIGURE 8 | **Equal area projections of the ChRM directions for all the studied sections before and after bedding correction. The 95% confidence ellipse for the normal and reverse mean directions is indicated. Statistical information is given (N, number of samples; Dec., declination; Inc., inclination: k Fisher's precision parameter; α_{95}, radius of the 95% confidence cone).**

marine sediments of the Vic area, is in disagreement with the previous published data, which limited the marine sedimentation to the late Bartonian larger foraminifer Zone *N. variolarius*/*incrassatus*, SBZ18 (Papazzoni and Sirotti, 1995; Serra-Kiel et al., 2003b).

The thickness of chron C16n.2n along the ~16 km transect represented by the studied sections confirms partly the results from Taberner et al. (1999) regarding the basin asymmetry during the latest stages of marine deposition. Indeed, the normal chron has the shortest thickness in the south (45 m in Collsuspina), 65 m in the Tona and Múnter section, 72 m in the Gurb section and about 270-290 m in the Sant Bartomeu del Grau section (Fig. 3). Our biostratigraphic data constraint this chron to be C16n.2n and not C17n as inferred by Taberner et al. (1999). Moreover, Taberner et al. (1999) also suggested the presence of additional chrons in the upper part of the marine succession in the Sant Bartomeu del Grau section where a thin reverse magnetozone was detected in the quarry section. Our detailed sampling along the same section certainly detects the presence of clear reverse samples in this interval (Fig. 3). An unambiguous reverse level has also been observed in the Gurb section (Fig. 3) in the upper part of chron C16n.2n, a few meters below the gypsum level (Fig. 3). The evaporite unit is not present in the Sant Bartomeu section where continental fluviatile red sandstones (Artés Fm) directly overlay the terminal complex above the reef unit but the thin reverse level could be equivalent. However, we do not interpret these directions as primary and regard them as diagenetic overprints related to the continentalization. In fact, the lowest continental deposits in the Múnter and Sant Bartomeu del Grau section hold a reverse magnetisation. Therefore we invoke a delayed diagenetic magnetisation to explain the thin reverse levels within the upper part of C16n.2n. Equivalent reverse levels have not been observed in the Múnter section whereas some anomalous weak discarded directions have been observed in the Collsuspina_2 section (Fig. 3). The relative short thickness of this contended reverse magnetozone (a few meters at the most) relative to the thickness of chron C16n.2n precludes interpreting it as a real chron. Note, that the duration of chron C16n.2n is 0.569 Ma and the reverse chron immediately above (C16n.1r) is 0.140 Ma, four times shorter than C16n.2n. Therefore, chron C16n.2n extends at least up to the evaporites and minimum sediment accumulation rates can be given for the uppermost marine succession in the Vic area as follow: 79 m/Ma at Collsuspina section, 65m/Ma at the Tona and Múnter sections, 72 m/Ma at the Gurb section and about 270-290 m/Ma at the Sant Bartomeu del Grau area. The position of the Bartonian/Priabonian boundary cannot be placed accurately since our chronology only reaches chron C16r. However, it could be inferred to lie within the interval extending from the lower part of the Vespella Mb down to the upper part of the Manlleu Mb considering overall sedimentation rates and previous magnetostratigrafies (Fig. 2).

CONCLUSIONS

The analyses of calcareous nannofossils revealed the presence of Priabonian marine sediments in the southeastern Pyrenean foreland basin. The studied sediments belong to the Zones NP18 and NP19-20 (Martini, 1971) on the basis of the occurrence of *C. oamaruensis* and *I. recurvus*, respectively. We challenge all previous chronostratigraphies for the uppermost marine sediments that assigned an upper Bartonian age to the uppermost marine sediments (Serra-Kiel et al, 2003 a and b) and a correlation to C17n.1n (Burbank et al, 1992, Taberner et al., 1999). Our current dataset assign the FO of *I. recurvus* close to the C16r/C16n.2n at a somewhat lower position than previous studies, and is in agreement with a proposed age of ~35 Ma for the Cardona evaporite unit by Taberner et al. (1999).

This study suggests a revision of the chronostratigraphy of the Vic area. Moreover, the occurrence of calcareous nannofossils from carbonate platform lithofacies, starting from the base of the succession, certainly will contribute to improve the direct correlations between larger foraminifer and planktic microfossil zones.

REFERENCES

Anadón, P., Feist, M., Hartenberger J-L., Muller, C., de Villalta-Comella, J., 1983. Un exemple de corrélation biostratigraphique entre échelles marines et continentales dans l'Eocène: la coupe de Pontils (bassin de l'Ebre, Espagne). Bulletin Société Géologique France, 25(5), 747-755.

Aubry, M.P., 1992. Late Paleogene calcareous nannoplankton evolution: a tale of climatic deterioration. In: Prothero, D. R., and Berggren, W. A. (eds.). Eocene-Oligocene climatic and biotic evolution. Princeton, Princeton University Press, 272-309.

Aubry, M.P., 1999. Handbook of Cenozoic calcareous nannoplankton. Book 2: Ortholithae (Holococcoliths, Ceratoliths, Ortoliths, and others). American Museum of Natural History, New York, Micropaleontological Press, 368 pp.

Berggren, W.A., Kent, D.V., Swisher, C.C.III, Aubry M.P., 1995. A revised Cenozoic Geochronology and Chronostratigraphy. In: Berggren, W.A., Kent, D.V., Aubry M.P. and Handerbol, J. (ed.). Geochronology, time scales and global stratigraphic correlation. Society Economic Paleontologists and Mineralogists, Special Publication, 54, 129-212.

Blow, W. H., 1969. Late middle Eocene to Recent planktonic foraminiferal biostratigraphy. In: Bronnimann, P.R., Renz, H.H. (eds.). Proceeding of the First International Conference on Planktonic microfossils, Geneva, 1, 199-421.

Bown, P.R., 1998. Calcareous Nannofossil Biostratigraphy. British Micropaleontological Society Publications Series, London, ed. Kluwer Academic Press, 315 pp.

Burbank, D.W., Puigdefàbregas, C., Muñoz, J.A., 1992. The chronology of the Eocene tectonic and stratigraphic development of the eastern Pyrenean Foreland Basin, NE Spain. Geological Society of America Bulletin, 104, 1101-1120.

Canudo, J.I., Molina, E., Riveline, J., Sucunza, M., 1988. Les événements biostratigraphiques de la zone prépyrénéenne d'Aragon (Espagne), de l'Eocène moyen à l'Oligocène inféreur. Revue de Micropaléontologie, 31, 15-29.

Catanzariti, R., Rio, D., Martelli, L., 1997. Late Eocene to Oligocene calcareous nannofossil biostratigraphy in Northern Apennines: the Ranzano Sandsone. Memorie di Scienze Geologiche, 49, 207-253.

Ferrer, J., 1971. El Paleoceno y Eoceno del borde suroriental de la Depresion del Ebro (Catalana). Mémoires suisses de Paléntologie, 90, 70 pp.

Fornaciari, E., Catanzariti, R., Rio, D., Agnini, C., Bolla, E.M., Valvasoni, E., 2006. Improving resolution of calcareous nannofossil biostratigraphy at the Middle to Late Eocene transition. Climate and Biota of the Early Paleogene, Bilbao, Volume of Abstracts, 44.

Gradstein, F., Ogg, J., Smith, A., 2004. A Geological Timescale 2004. New York, Cambridge University Press, 589 pp.

Jovane, L., Sprovieri, M., Florindo, F., Acton, G.D., Coccioni, R., Dall'Antonia, B., Dinarès-Turell, J., 2007. Eocene-Oligocene paleoceanographic changes in the stratotype section, Massignano, Italy: clues from rock magnetism and stable isotopes. Journal Geophysical Research, 112, B11101, doi:10.1029/ 2007JB004963.

Kirschvink J.L., 1980. The least-squares line and plane and the analysis of palaeomagnetic data, Geophys. Journal Royal Astronomical Society 62, 699–718.

Luciani, V., Negri, A., Bassi, D., 2002. The Bartonian-Priabonian transition in the Mossano section (Colli Berici, northeastern Italy): a tentative correlation between calcareous plankton and shallow-water benthic zonations. Geobios, Mémoire special, 24, 140-149.

Luterbacher, H., 1998. Sequence stratigraphy and the limitations of biostratigraphy in the marine Paleogene Strata of the Tremp basin (central part of the Southern Pyrenean foreland basin, Spain). In: Hardenbol, J., Jacquin, T., Vail, P.R. (eds). Mesozoic and Cenozoic sequence stratigraphy of European basin. Society Economic Paleontologists and Mineralogists, Special Publication, 60, 303-309.

Marino, M., Flores, J.-A., 2002. Middle Eocene to Early Oligocene calcareous nannofossil stratigraphy at Leg 177 Site 1090. Marine Micropaleontology, 45, 383-398.

Martini, E., 1971. Standard Tertiary and Quaternary calcareous nannoplankton zonation. In: Farinacci, A. (ed.). Proceedings of the Second Planktonic Conference Roma 1970. Roma, Edizioni Tecnoscienza, 2, 739-785.

McFadden, P.L., McElhinny, M.W., 1990. Classification of the reversal test in paleomagnetism. Geophysical Journal International, 103, 725-729.

Nocchi, M., Parisi, G., Monaco, P., Monechi, S., Madile, M., 1988. Eocene and Early Oligocene micropaleontology and

paleoenvironments in SE Umbria, Italy. Palaeography, Palaeoclimatology, Palaeoecology, 67, 181-244.

Okada, H., Bukry, D., 1980. Supplementary modification and introduction of code numbers to the low-latitutde coccolith biostratigraphic zonation (Bukry, 1973; 1975). Marine Micropaleontology, 5, 321-325.

Papazzoni, C.A., Sirotti, A., 1995. Nummulite biostratigraphy at Middle/Upper Eocene boundary in the Northern Mediterranean area. Rivista Italiana di Paleontologia e Stratigrafia, 101, 63-80.

Persico, D., Villa, G., 2004. Eocene-Oligocene calcareous nannofossils from Maud Rise and Kerguelen Plateau (Antartica): paleoecological and paleoceanographic implications. Marine Micropaleontology, 52, 153-179.

Perch-Nielsen, K., 1985. Cenozoic calcareous nannofossili. In: Bolli, H.M., Saunders, J.B., Perch-Nielsen, K. (eds.). Plankton Stratigraphy. Cambridge, Cambridge University Press, 427-554.

Pisera, A., Busquets, P., 2002. Eocene siliceous sponges from the Ebro Basin (Catalonia, Spain). Geobios, 35, 321.

Reguant, S., 1967. El Eoceno Marino de Vic (Barcelona). Memorias del Instituto Geológico y Minero de España, 68, 350 pp.

Riba, O., 1967. Resultados de un estudio sobre el Terciario continental de la parte Este de la depresión central catalana. Acta Geologica Hispanica, 2(1), 3-8.

Riba, O., 1975. Le Bassin tertiaire Catalan Espagnol et les gisements de potasse. Ixe. Congrès International de Sédimentologie, Nice. Exursión Guidebook nº 20, 9-13.

Rio, D., Premoli-Silva, I., Agnini, C., Brinkhuis, H., Fornaciari, E., Giusberti L., Grandesso, P., Lanci, L., Lucani, V., Mattoni, G., Stefani, C., Villa, I., 2006. The Alano di Piave, section (Venetian Southern Alps, NE Italy). A potential GSSP of the Priabonian stage (Upper Eocene). Climate and Biota of the Early Paleogene, Bilbao, Volume of Abstract, 109.

Romero, J., Caus, E., 2000. Eventos Neríticos en el límite Eoceno Medio-Eoceno Superior en el extremo oriental de la depresión del Ebro (NE de España). Revista de la Sociedad Geológica de España, 13(2), 301-321.

Serra- Kiel, J., Busquets, P., Travé, A., Mató, E., Saula, E., Tosquella, J., Samsó, J.M., Ferràndez, C., Barnolas, A., Àlvarez-Pérez, G., Franquès, F., Romero, J., 1997. Field Trip Guide. 2nd Meeting IGCP 393 Neritic Events at the Middle-Upper Eocene Boundary, 51 pp.

Serra-Kiel, J., Hottinger, L., Caus, E., Drobne, K., Ferràndez, C., Jauhri, A.K., Less, G., Pavlovec, R., Pignatti, J., Samsó, J.M., Schaub, H., Sirel, E., Strougo, A., Tambareau, Y., Tosquella, J., Zakrevskaya, E., 1998. Larger Foraminiferal Biostratigraphy of the Tethyan Paleocene and Eocene. Bulletin de la Societé Géeologique de France, 169(2), 281-299.

Serra-Kiel, J., Travé, A., Mató, E., Saula, E., Ferràndez-Cañadell, C., Busquets, P., Tosquella, J., Vergés, J., 2003a. Marine and transitional Middle/Upper Eocene Units of the Southern Pyrenean Foreland Basin (NE Spain). Geologica Acta, 1(2), 177-200.

Serra-Kiel, J., Mató, E., Saula, E., Travé, A., Ferràndez-Cañadell, C., Busquets, P., Samsó, J.M., Tosquella, J., Vergés, J., Barnolas, A., Àlvarez-Pérez, G., Franquès, J., Romero, J., 2003b. An inventory of the marine and transitional Middle/Upper Eocene deposits of the Southeastern Pyrenean Foreland Basin (NE Spain). Geologica Acta, 1(2), 177-200.

Serra-Kiel, J., Ferràndez-Cañadell, C., Cabrera, L., Marzo, M., Busquets, P., Colombo, F., Reguant, S., 2003c. Discussion and replay: Basin infill architecture and evolution from magnetostratigraphy cross-basin correlations in the southeastern Pyrenean foreland basin. Geological Society of America Bulletin, 15, 249-252.

Taberner, C., Dinarès-Turell, J., Giménez, J., Docherty, C., 1999. Basin infill architecture and evolution from magnetostratigraphy cross-basin correlations in the southeastern Pyrenean foreland basin. Geological Society of America Bulletin, 11, 1155-1174.

Taberner, C., Dinarès-Turell, J., Giménez, J., Docherty, C., 2003. Discussion and replay: Basin infill architecture and evolution from magnetostratigraphy cross-basin correlations in the southeastern Pyrenean foreland basin. Geological Society of America Bulletin, 15, 253-256.

Varol, O., 1998. Palaeogene. In: Bown, P.R., (ed.). Calcareous Nannofossil Biostratigraphy. British Micropaleontological Society Publications Series, London, ed. Kluwer Academic Press, 315 pp.

Verducci, M., Nocchi, M., 2004. Middle to Late Eocene main planktonic foraminiferal events in the Central Mediterranean area (Umbria-Marche basin) related to paleoclimatic changes. Neus Jahrbuch fur Geologie und Paleontologie Abhandlungen, 234(1-3), 361-413.

Zijderveld, J.D.A., 1967. AC demagnetization of rock: analysis of results. In: Collinson, D.W., Creer, K.M., Runcorn, S.K. (eds.). Methods in palaeomagnetism. Amsterdam, Elsevier, pp. 254-286.

Manuscript received November 2007;
revision accepted February 2008;
published Online November 2008.

APPENDIX

Calcareous nannofosil distribution in the studied sections

TABLE 1 | **Calcareous nannofossil distribution of the Collsuspina 1-2 sections.**

SAMPLES	LEVEL (metres)	Total abundance[a]	Preservation[b]	Reworking	*Braarudosphaera bigelowii*	*Coccolithus pelagicus*	*Sphenolithus* spp.	*Discoaster* spp.	*Pontosphaera* spp.	*Zygrhablithus bijugatus*	*Coccolithus formosus*	*Helicosphaera* spp.	*Discoaster barbadiensis*	*Cyclicargolithus floridanus*	*Reticulofenestra* spp.	*Coccolithus eopelagicus*	*Pseudotriquetrorhabdulus inversus*	*Lanternithus minutus*	*Dictyococcites* spp.	*Reticulofenestra umbilica*	*Calcidiscus protoanulus*	*Clausicoccus subdistichus*	*Reticulofenestra daviesi*	*Cribrocentrum reticulatum*	*Discoaster saipanensis*	*Helicosphaera compacta*	*Sphenolithus predistentus*	*Dictyococcites bisectus*	*Helicosphaera euphratis*	*Isthmolithus recurvus*	NANNOFOSSIL ZONE	AGE
CP7-2	46,0	B		.	.	.	.	.	.	.	.	.	.	.	.	.	.	.	.	.	.	.	.	.	.	.	.	.	.	.	.	NP19 - NP 20	PRIABONIAN
CP6-2	44,0	B		.	.	.	.	.	.	.	.	.	.	.	.	.	.	.	.	.	.	.	.	.	.	.	.	.	.	.	.		
CP5-1	42,0	F	M/P	.	.	C	R	.	P	P	.	.	.	A	.	R	.	F	F	.	R	P	.	.	.	P	.	C	P	.		
CP4-2	40,0	C	M	.	.	C	F	.	R	.	.	.	R	A	.	F	.	F	F	.	.	R	.	.	R	R	.	C	.	.		
CP3-1	37,0	C	M	.	.	A	R	.	R	.	R	.	R	A	.	C	.	F	R	.	R	R	.	.	.	R	.	R	.	P		
CP2-1	33,0	F	M/P	.	.	A	R	.	R	R	.	.	.	A	.	F	.	F	.	.	.	.	.	R	.	.	.	F	.	.		
CP1-1	30,0	C	M/P	.	.	C	F	.	P	F	.	.	.	A	.	F	.	F	C	P	.	.	.	.	P	.	.	C	.	P		
CS15	20,0	C	M	P	P	F	R	.	R	R	P	.	.	A	.	R	R	F	F	.	.	R	.	R	.	.	P	R	P	.	NP18 (?)	Priabonian (?)
CS14	15,0	F	M/P	P	.	C	R	.	.	F	F	.	.	C	.	C	.	F	F	.	.	.	.	.	.	.	.	C	.	.		
CS13	10,0	F	M/P	P	.	C	F	.	R	P	F	.	.	A	.	F	.	R	C	.	P	P	.	R	.	.	.	R	.	.		
CS12	5,0	R	M	.	.	C	.	.	.	.	F	.	.	C	.	F	.	F	R	.	.	.	.	R	.	.	.	R	.	.		
CS11	0,0	F	M/P	P	.	C	R	.	P	R	F	.	P	C	R	R	.	F	C	R	.	R	P	R	.	.	.	F	.	.		
CO4	55,0	F	M/P	.	.	C	F	.	▫	F	R	.	.	A	.	R	.	C	R	.	.	R	.	R	.	.	.	F	.	.		
CO3A	54,0	C	P/M	.	R	C	R	R	R	R	R	.	R	A	.	R	.	C	R	R	.	R	.	F	.	.	.	C	.	.		
CO3	53,0	F	P/M	.	P	C	R	R	F	F	R	.	.	C	.	R	.	C	F	.	R	R	.	F	P	.	.	F	.	.		
CO2	23,0	C	M/P	.	P	C	F	R	.	F	.	P	.	F	R	R	.	A	F	.	R	P	.	F	.	.	.	F	.	.		
CO1	0,0	C	M/P	P	R	F	P	R	R	F	R	.	.	F	R	R	R	A	R	.	.	.	.	C	.	.	.	F	.	.		

(a): **A** (abundant): >30 spec.s for view; **C** (common): 10 to 30 spec.s for view; **F** (few): 1 to 10spec.s for view; **R** (rare): 0.1- 1 spec.s for view; **P** (presence): < 0.1spec.s for view; **B** (barren): no specimens. The abundance classes for the single species and the reworking are as follows: A (abundant): >30%; C (common): 10 to 30%; F (few): 1 to 10%; R (rare): 0.1-1 %; P (presence): < 0.1%.

(b)**: G** (good): little or no evidence of dissolution and/or secondary overgrowth; fully preserved diagnostic characters. **M** (moderate): dissolution and/or secondary overgrowth; partially altered primary morphological characteristics; nearly all specimens can be identified at the species level. **P** (poor): severe dissolution, fragmentation and/or secondary overgrowth; largely destroyed primary features; many specimens cannot be identified at the species and/or at generic level.

TABLE 2 | **Calcareous nannofossil distribution of the Tona section.**

SAMPLES	LEVEL (metres)	Total abundance[a]	Preservation[b]	Reworking	*Braarudosphaera bigelowii*	*Coccolithus pelagicus*	*Sphenolithus* spp.	*Pontosphaera* spp.	*Zygrhablithus bijugatus*	*Coccolithus formosus*	*Helicosphaera* spp.	*Discoaster barbadiensis*	*Cyclicargolithus floridanus*	*Helicosphaera lophota*	*Reticulofenestra* spp.	*Coccolithus eopelagicus*	*Lanternithus minutus*	*Dictyococcites* spp.	*Reticulofenestra umbilica*	*Calcidiscus protoanulus*	*Clausicoccus subdistichus*	*Reticulofenestra daviesi*	*Cribrocentrum reticulatum*	*Pontosphaera obliquipons*	*Discoaster saipanensis*	*Helicosphaera compacta*	*Sphenolithus predistentus*	*Discoaster tanii*	*Helicosphaera bramlettei*	*Dictyococcites bisectus*	*Helicosphaera euphratis*	*Chiasmolithus oamaruensis*	*Isthmolithus recurvus*	NANNOFOSSIL ZONE	AGE
TO22D	70,0	C	M		R	C	.	R	R	.	.	R	C	.	.	C	F	F	.	.	R	P	R	.	R	P	.	.	P	C	R	.	.	NP19 - NP20	PRIABONIAN
TO22C	65,0	C	M/P		.	F	R	F	.	F	.	.	A	.	.	C	F	F	.	.	R	.	R	.	.	.	.	.	.	R	.	.	P		
TO22B	60,0	C	M/P		P	C	F	R	R	R	.	.	A	.	R	R	C	R	R	.	R	.	R	.	R	.	.	.	.	F	.	.	.		
TO22A	58,0	F	M/P	P	P	C	F	R	F	F	.	.	C	.	.	C	F	F	P	P	P	.	F	.	.	.	P	.	.	C	.	.	P		
TO22	55,0	C	M/P	P	P	F	R	P	F	R	.	P	C	.	.	C	C	F	P	P	P	.	R	.	P	P	P	.	P	R	.	P	P		
TO21C	53,0	F	M/P		.	C	.	P	.	R	.	.	A	.	.	F	F	F	.	.	R	.	F	.	.	.	.	.	.	R	.	.	.		
TO21B	50,0	C	M/P	P	R	F	P	P	R	F	.	.	C	.	.	C	C	R	P	P	R	R	R	.	P	.	P	.	P	P	P	.	.		
TO21A	47,0	F	M/P		.	C	P	R	R	R	.	.	A	.	.	C	C	R	.	.	P	.	R	.	.	.	.	.	.	.	P	.	.		
TO21	44,0	F	P	P	P	F	R	P	R	F	.	.	A	.	.	F	C	.	P	P	P	.	P	.	P	.	.	P	P	R	.	.	.		
TO20A	37,0	C	M	P	P	C	R	P	F	P	.	.	F	.	.	R	C	F	P	P	F	.	F	.	.	P	.	.	.	F	.	P	P		
TO20	31,0	C	M/P		.	C	R	P	.	P	.	.	C	.	.	C	C	F	R	P	.	.	F	.	.	P	.	.	P	F	.	.	.	NP18 (?)	Priabonian (?)
TO19A	25,0	F	M/P	P	P	C	R	P	F	P	.	P	F	.	.	R	A	F	P	R	F	R	.	.	P	.	.	.	P	F	P	.	.		
TO19	22,0	F	P	P	P	C	F	R	.	F	.	.	C	.	.	F	C	F	P	P	P	P	F	.	.	.	.	.	.	C	.	.	.		
TO18	16,0	C	M	P	P	F	R	.	R	R	.	.	F	.	.	.	A	F	P	P	P	P	C	.	.	.	.	.	.	F	P	.	.		
TO17	11,0	F	M	P	P	F	R	P	F	.	.	.	F	.	.	P	A	F	.	.	P	P	F	.	.	.	.	.	.	F	.	.	.		
TO16	3,0	C	M	P	.	F	R	P	F	P	P	.	C	R	R	P	A	F	P	.	P	.	F	.	P	P	.	.	P	F	.	.	.		
TO15B	2,0	F	M	P	.	F	R	.	F	R	.	.	C	.	.	P	A	F	.	.	P	R	F	.	P	P	.	.	.	F	.	.	.		
TO15A	1,0	F	M	P	.	F	R	R	F	R	.	.	C	.	.	P	A	F	.	.	.	.	C	.	.	P	.	.	.	F	.	.	.		
TO15	0,0	C	M	P	P	F	R	P	R	P	.	.	C	.	R	P	A	P	P	.	.	R	F	.	.	.	.	.	.	F	.	.	.		

TABLE 3 | **Calcareous nannofossil distribution of the Munter 1-2 sections.**

SAMPLES	LEVEL (metres)	Total abundance[a]	Preservation[b]	Reworking	*Braarudosphaera bigelowii*	*Coccolithus pelagicus*	*Chiasmolithus* spp.	*Sphenolithus* spp.	*Discoaster* spp.	*Pemma sp.*	*Pontosphaera* spp.	*Zygrhablithus bijugatus*	*Coccolithus formosus*	*Helicosphaera* spp.	*Discoaster barbadiensis*	*Cyclicargolithus floridanus*	*Helicosphaera lophota*	*Reticulofenestra* spp.	*Coccolithus eopelagicus*	*Pseudotriquetrorhabdulus inversus*	*Lanternithus minutus*	*Dictyococcites* spp.	*Reticulofenestra umbilica*	*Calcidiscus protoanulus*	*Clausicoccus subdistichus*	*Reticulofenestra daviesi*	*Cribrocentrum reticulatum*	*Pontosphaera obliquipons*	*Discoaster saipanensis*	*Helicosphaera compacta*	*Sphenolithus predistentus*	*Discoaster tanii*	*Helicosphaera bramlettei*	*Dictyococcites bisectus*	*Helicosphaera euphratis*	*Chiasmolithus oamaruensis*	*Isthmolithus recurvus*	NANNOFOSSIL ZONE	AGE
MTN15/1	65,0	P	M/P	P	.	P	.	.	.	.	.	.	P	.	.	P	.	.	.	.	.	P	.	.	.	.	P	.	.	.	.	.	.	.	.	.	.	NP19 - NP20	PRIABONIAN
MTN14	62,0	F	M/P	R	R	A	.	R	R	R	R	R	F	R	R	C	R	P	R	.	F	R	R	R	R	.	R	.	R	P	.	.	R	F	.	.	.		
MTN13	57,0	F	M	R	.	C	.	P	.	.	R	.	.	R	.	C	.	.	C	.	R	.	.	P	F	.	.	.	P	P	.	.	.	R	.	.	.		
MTN12	55,0	C	M/P	R	P	C	.	R	R	R	P	F	F	P	.	A	R	R	R	.	R	F	R	R	R	R	P	.	R	P	.	.	P	C	P	.	.		
MTN11	50,0	C	M	R	P	C	.	R	.	.	.	R	F	.	.	A	.	.	F	P	R	R	.	P	R	.	R	.	.	R	.	.	.	C	.	.	.		
MTN10	45,0	C	M	R	P	F	.	P	R	R	R	F	R	.	.	A	R	R	F	P	R	R	R	R	R	P	R	P	P	P	.	.	.	F	.	.	.		
MTN9	40,0	C	M	R	P	F	.	P	.	.	.	F	.	.	.	A	.	R	.	P	F	C	R	P	F	P	P	P	R	.	.	.	.	F	.	.	.		
MTN8	35,0	C	M	R	.	F	R	.	.	F	F	R	.	.	.	C	.	.	.	R	F	C	R	R	.	.	R	R	R	.	.	.	.	C	.	.	.		
MTN7	30,0	C	M/P	R	P	C	.	F	.	.	R	F	R	.	P	C	.	.	F	.	F	F	R	P	P	.	R	F	R	.	.	.	.	F	.	.	.		
MTN6	25,0	C	M/P	R	.	C	.	F	.	.	.	F	R	.	R	C	.	.	.	.	C	C	R	.	.	.	R	R	R	R	.	.	.	C	.	.	.		
MTN5	20,0	C	M/P	F	R	C	.	F	.	.	R	.	R	.	.	A	R	.	R	.	C	C	R	R	.	.	R	R	.	.	.	.	R	F	.	.	.		
MTN4	14,0	C	M/P	R	R	F	.	R	R	.	R	R	R	R	.	C	.	.	R	R	C	C	R	R	R	.	R	.	R	R	.	.	R	F	.	.	.		
MTN3	10,0	C	M	R	.	C	.	F	.	.	R	R	R	.	R	C	R	R	.	.	C	F	R	R	F	.	F	.	R	R	R	.	.	R	.	.	P		
MUN22	48,0	F	M	R	.	C	.	R	.	.	.	R	R	.	.	F	.	.	R	.	C	C	.	R	F	F	F	.	.	.	.	.	.	C	.	.	.		
MUN21	43,0	C	M	R	R	C	.	F	R	R	R	R	R	R	R	C	R	.	R	.	C	R	R	R	R	.	F	.	R	P	.	.	R	C	.	.	P		
MUN15	40,0	C	M	R	R	C	.	R	R	R	R	R	R	R	.	C	R	R	R	.	C	C	R	R	R	.	F	.	R	P	.	.	R	F	.	.	.		
MUN18	37,0	F	M	R	.	F	.	R	P	.	R	R	R	.	.	R	.	F	R	R	C	F	P	P	R	R	.	.	.	.	.	.	P	F	.	.	.	NP18	
MUN19	33,0	C	M	R	R	F	.	R	.	.	P	R	P	.	.	F	.	.	.	R	C	C	.	F	.	P	F	R	P	R	.	.	.	F	.	.	.		
MUN20	30,0	F	M	R	.	C	.	.	.	.	.	R	.	.	.	C	.	.	.	.	C	F	.	R	.	P	F	R	.	.	.	.	.	C	.	.	.		
MUN14	25,0	C	M	R	R	C	.	F	R	R	R	R	R	R	C	R	.	R	.	C	R	R	R	R	.	R	.	R	P	.	.	R	F	.	.	.		
MUN12	21,0	C	M	R	.	F	.	F	R	R	R	F	R	.	.	C	R	R	R	.	F	F	R	R	.	R	F	.	R	R	.	.	.	C	.	.	.		
MUN10	17,0	C	M	R	.	F	.	F	R	R	R	F	R	.	.	C	R	R	R	.	A	F	R	R	.	R	F	.	R	.	.	.	.	F	.	.	.		
MUN7	11,0	C	M/P	R	.	F	.	F	R	R	R	F	R	.	.	C	R	R	R	.	A	F	R	R	.	R	F	.	R	.	.	.	.	F	.	.	.		
MUN5	7,0	C	M	R	R	C	.	R	.	.	R	F	R	.	.	A	.	R	.	.	C	C	R	R	.	.	F	.	R	.	.	.	.	C	.	P	.		
MUN4	5,0	C	M	R	R	C	.	R	R	.	R	F	R	R	.	F	.	.	R	R	A	F	R	R	R	R	R	.	.	.	.	R	R	R	.	R	.		

See explanation in pg. 295

TABLE 4 | **Calcareous nannofossil distribution of the Gurb section.**

SAMPLES	LEVEL (meters)	Total abundance[a]	Preservation[b]	Reworking	*Braarudosphaera bigelowii*	*Coccolithus pelagicus*	*Sphenolithus* spp.	*Discoaster* spp.	*Pontosphaera* spp.	*Rhabdosphaera* spp.	*Zygrhablithus bijugatus*	*Coccolithus formosus*	*Helicosphaera* spp.	*Discoaster barbadiensis*	*Cyclicargolithus floridanus*	*Reticulofenestra* spp.	*Coccolithus eopelagicus*	*Pseudotriquetrorhabdulus inversus*	*Pemma* spp.	*Lanternithus minutus*	*Dictyococcites* spp.	*Reticulofenestra umbilica*	*Calcidiscus protoanulus*	*Clausicoccus subdistichus*	*Reticulofenestra daviesi*	*Cribrocentrum reticulatum*	*Pontosphaera obliquipons*	*Discoaster saipanensis*	*Helicosphaera compacta*	*Sphenolithus predistentus*	*Discoaster tanii*	*Helicosphaera bramlettei*	*Dictyococcites bisectus*	*Helicosphaera euphratis*	*Chiasmolithus oamaruensis*	*Isthmolithus recurvus*	NANNOFOSSIL ZONE	AGE
GUR18	58,8	C	M	R	P	A	P	P	R	.	R	P	.	.	F	R	R	.	P	R	C	.	.	F	.	.	P	.	.	.	.	.	P	.	.	P	NP 19 - NP 20	PRIABONIAN
GUR17	55,6	C	M	P	R	C	R	R	P	.	R	F	R	.	F	R	F	.	P	F	A	P	P	R	.	.	P	R	P	P	.	P	C	.	.	.		
GUR16	53,0	C	M	P	R	C	R	R	P	.	R	R	R	.	F	R	F	.	.	F	A	P	.	R	.	P	.	R	P	P	.	.	C	.	P	.		
GUR15	50,9	C	M		.	C	P	P	P	.	P	P	P	.	F	R	F	.	.	F	A	.	P	R	.	R	.	P	.	.	.	.	C	.	.	P		
GUR14	48,7	F	M/P	P	.	C	.	P	P	P	R	P	.	.	P	P	R	.	.	C	A	P	P	R	P	P	P	.	.	.	.	.	R	.	.	.		
GUR13	46,6	F	M/P		.	F	R	P	.	.	R	P	.	.	R	P	.	P	P	F	A	.	.	.	P	P	.	.	.	.	.	.	F	.	.	.		
GUR12	44,2	C	M	R	P	F	R	R	R	.	R	R	R	.	F	R	R	P	.	F	A	R	R	R	.	F	R	P	P	.	.	.	R	.	.	.		
GUR11	42,2	C	M/P		P	C	R	R	R	P	R	R	P	.	R	R	R	.	.	F	A	P	P	R	.	R	P	P	P	.	.	.	F	.	.	.		
GUR10	39,2	C	M/P		P	C	R	R	R	.	F	R	P	.	R	R	F	.	.	F	A	P	P	R	.	P	.	P	.	.	.	P	F	.	.	.		
GUR9	37,2	C	M/P	R	P	C	R	P	R	P	R	R	P	.	R	R	R	R	.	C	A	P	P	R	.	P	.	P	.	.	.	P	C	.	.	.		
GUR8	35,8	C	M		R	F	R	R	P	.	R	R	R	.	R	R	F	.	.	C	A	P	R	R	.	F	.	P	.	.	.	.	R	.	.	.		
GUR7	33,7	C	M/P		.	F	R	R	P	.	R	R	.	P	R	.	.	.	.	C	A	P	P	P	P	R	P	P	.	P	P	P	F	.	.	.		
GUR6	31,8	C	M/P		P	F	R	P	P	.	P	P	.	P	R	.	R	P	.	C	A	P	.	P	.	P	.	.	.	.	.	.	F	P	.	.		
GUR5	29,5	C	M/P		P	F	R	P	P	.	R	R	.	.	R	P	R	.	.	C	C	P	R	R	P	R	.	R	P	P	.	.	C	P	P	.		
GUR4	27,9	C	M		P	F	P	P	P	.	R	R	.	.	R	P	R	.	.	C	C	P	P	R	P	P	.	P	P	.	.	.	C	.	.	.		
GUR3	26,6	C	M	P	P	F	R	P	P	.	R	P	.	.	R	P	P	P	.	C	C	P	R	R	P	P	P	P	P	.	P	.	C	P	.	.		
GUR2	24,4	C	M		.	F	R	P	P	.	R	P	.	.	R	P	P	P	P	C	F	P	.	P	.	F	P	.	P	.	.	.	F	.	.	P		
GUR1	24,0	F	M	P	P	F	R	P	P	.	P	P	.	.	R	P	P	P	.	C	F	.	P	P	.	C	.	P	.	P	.	.	F	.	.	.		
GUR20	21,0	C	M	P	P	C	R	P	P	.	F	R	P	.	.	.	R	.	.	C	C	P	R	F	.	F	P	P	P	P	.	.	R	.	.	P		
GUR22	20,5	C	M/P	R	P	F	R	.	R	.	R	R	R	P	C	.	R	P	.	C	C	.	F	F	.	F	P	R	.	P	.	.	R	.	.	.		
GUR24	18,0	C	M/P		.	F	R	.	.	.	F	R	.	.	C	R	P	P	P	C	C	P	R	F	.	R	P	.	P	R	.	.	R	.	.	R		
GUR26	17,0	C	M/P	P	P	C	F	.	.	.	R	P	.	.	C	R	R	.	.	C	F	P	P	F	.	C	.	.	.	.	.	.	F	.	.	R		
GUR29	14,5	C	M		.	C	R	.	.	.	R	R	R	.	A	R	F	.	.	F	F	R	R	F	.	R	R	R	P	.	.	R	F	.	.	P		
GUR31	12,0	C	M		.	C	R	.	.	.	R	R	.	.	A	R	F	.	.	F	F	R	R	C	.	R	.	.	.	.	.	R	R	.	.	R		
GUR33	10,0	C	M/P	R	.	C	F	.	P	.	F	F	.	.	C	.	F	.	.	F	R	P	P	F	R	F	P	P	.	P	.	.	C	.	.	P		
GUR34	8,5	C	M/P		.	C	R	.	R	.	R	F	R	R	C	R	R	.	.	C	C	R	R	R	R	F	.	R	.	.	.	.	C	.	.	.		
GUR35	5,6	F	M/P		P	C	R	.	.	.	R	R	P	P	C	P	.	.	.	R	F	P	R	F	.	R	.	P	P	.	.	.	F	.	P	.		
GUR36	4,7	F	M/P	R	.	C	F	.	.	.	R	F	R	.	A	R	R	.	.	C	F	R	R	F	R	F	.	.	.	.	.	.	C	.	.	.		
GUR37	3,5	C	M		.	C	R	.	P	.	P	R	.	.	A	.	.	.	.	F	F	P	P	F	.	F	.	.	P	.	.	P	C	.	.	P		
GUR38	3,0	C	M/P	R	R	C	R	R	R	.	F	R	.	R	C	R	.	.	.	F	C	R	R	F	R	F	.	.	.	.	.	.	C	.	R	P		
GUR40	1,5	F	M/P		R	F	F	R	.	.	R	R	.	.	C	.	.	.	.	C	C	.	.	.	.	C	.	.	.	.	.	.	C	.	.	.	NP18 (?)	Priab.(?)
GUR39	0,0	C	M		.	R	R	R	R	.	F	R	R	.	C	.	.	R	R	A	F	.	.	.	.	C	.	.	.	.	.	.	F	.	.	.		

(a): **A** (abundant): >30 spec.s for view; **C** (common): 10 to 30 spec.s for view; **F** (few): 1 to 10spec.s for view; **R** (rare): 0.1- 1 spec.s for view; **P** (presence): < 0.1spec.s for view; **B** (barren): no specimens. The abundance classes for the single species and the reworking are as follows: A (abundant): >30%; C (common): 10 to 30%; F (few): 1 to 10%; R (rare): 0.1-1 %; P (presence): < 0.1%.

(b)**: G** (good): little or no evidence of dissolution and/or secondary overgrowth; fully preserved diagnostic characters. **M** (moderate): dissolution and/or secondary overgrowth; partially altered primary morphological characteristics; nearly all specimens can be identified at the species level. **P** (poor): severe dissolution, fragmentation and/or secondary overgrowth; largely destroyed primary features; many specimens cannot be identified at the species and/or at generic level.

TABLE 5 | **Calcareous nannofossil distribution of the Sant Bartomeu del Grau section.**

SAMPLES	LEVEL (metres)	Total abundance[a]	Preservation[b]	Reworking	*Braarudosphaera bigelowii*	*Coccolithus pelagicus*	*Sphenolithus* sp.	*Discoaster* spp.	*Pontosphaera* spp.	*Zygrhablithus bijugatus*	*Coccolithus formosus*	*Helicosphaera* spp.	*Discoaster barbadiensis*	*Cyclicargolithus floridanus*	*Helicosphaera lophota*	*Reticulofenestra* spp.	*Pontosphaera multipora*	*Cocolithus eopelagicus*	*Pseudotrquetrorhabdulus inversus*	*Pemma* spp.	*Lanternithus minutus*	*Dictyococites hesslandii*	*Reticulofenestra umbilica*	*Clausicoccus subdistichus*	*Cribrocentrum reticulatum*	*Pontosphaera obliquipons*	*Sphenolithus predistentus*	*Discoaster saipanensis*	*Helicosphaera compacta*	*H. bramlettei*	*Dictyococites bisectus*	*Helicosphaera euphratis*	*Chiasmolithus oamaruensis*	*Isthmolithus recurvus*	NANNOFOSSIL ZONE	AGE
BGN16	333,0	R	M/P	R	R	R	.	.	.	P	R	.	.	R	.	.	.	.	.	.	R	.	.	.	P	.	.	P	.	.	P	.	.	.	NP19 - NP20	PRIABONIAN
BGN14	324,0	F	M/P	F	R	C	F	.	.	P	C	.	.	A	.	.	.	.	.	.	R	F	.	.	P	.	.	R	.	.	P	.	P	.		
BGN20	321,0	F	M/P	F	.	C	F	.	.	P	C	.	.	A	.	.	.	.	.	.	R	F	.	.	P	.	.	R	.	.	P	.	P	P		
BGN10	317,0	F	M/P	F	.	C	F	.	.	P	C	.	.	A	.	.	.	.	.	.	R	F	.	.	P	.	.	R	.	.	P	.	.	P		
BGN7	315,0	F	M/P	F	.	F	R	F	P	.	F	.	.	C	.	P	.	.	.	.	.	R	.	.	.	.	.	P	.	.	.	.	.	P		
BGN4	309,0	R	M/P	R	R	R	.	R	.	P	R	.	.	R	.	.	.	.	.	.	.	R	.	.	P	.	.	.	.	.	.	.	.	.	NP18 (?)	Priabonian (?)
BGN2	307,0	P	P/M	P	P	P	.	P	.	P	P	.	.	P	.	.	.	.	.	.	.	P	.	.	.	.	.	.	.	.	.	.	.	.		
BGN1	305,5	P	P/M	P	P	P	.	P	.	P	P	.	.	P	.	.	.	.	.	.	.	P	.	.	.	.	.	.	.	.	.	.	.	.		
SBN16	304,0	F	P	R	P	F	R	R	.	R	R	.	.	F	.	.	P	.	.	.	.	R	.	.	.	.	.	.	.	.	.	.	.	.		
SBN14	302,0	F	M/P	R	P	F	F	F	.	F	F	P	.	A	.	.	.	.	.	P	P	F	.	.	.	.	.	.	.	.	P	.	.	.		
SBN11	300,0	P	P		.	P	.	.	.	.	.	.	.	P	.	.	.	.	.	.	.	P	.	.	.	.	.	.	.	.	.	.	.	.		
SBN9	287,0	P	P		.	P	.	.	.	.	.	.	.	P	.	.	.	.	.	.	.	P	.	.	.	.	.	.	.	.	.	.	.	.		
SBN8	277,0	P	P		.	P	.	.	.	.	.	.	.	P	.	.	.	.	.	.	.	P	.	.	.	.	.	.	.	.	.	.	.	.		
SBN6	267,0	F	P/M	R	R	C	F	R	.	R	R	P	.	A	.	.	.	.	.	.	P	.	.	.	.	.	.	P	.	.	.	.	.	.		
SBN4	257,0	F	M/P	R	.	C	.	.	P	R	P	.	.	A	.	.	P	P	.	P	R	R	.	.	.	.	.	.	.	.	P	.	.	.		
SBN3	255,0	F	P/M	R	.	C	.	.	P	R	P	.	.	A	.	.	P	P	.	P	R	R	.	.	.	.	.	.	.	.	P	.	.	.		
SBN2	253,0	F	P/M	R	P	C	R	R	.	R	F	.	.	C	P	.	.	P	.	P	R	F	.	P	.	.	.	.	.	.	.	.	.	.		
SBN1	250,0	R	M/P		R	R	R	.	.	R	R	.	R	R	.	.	.	.	.	P	R	R	.	.	.	.	.	.	.	.	.	.	.	.		
SBGN14/1	236,0	F	P/M		R	F	R	.	F	F	R	.	.	A	.	R	.	.	.	.	C	R	.	R	R	.	.	.	R	.	.	.	.	.		
SBGN14/2	234,0	R	M/P		R	C	R	.	R	R	R	.	.	A	.	.	.	.	.	.	C	F	.	.	F	.	.	.	R	.	.	.	.	.		
SBGN13	230,0	R	M/P	R	R	C	R	.	.	R	.	.	.	A	.	R	.	.	.	.	F	F	R	.	R	.	.	.	.	.	F	.	.	.		
SBGN12	226,0	F	M/P	R	.	A	R	.	.	F	F	.	.	A	.	R	.	.	.	.	F	R	R	.	F	.	.	.	.	.	.	.	.	.		
SBGN11	222,0	R	M/P	F	.	C	F	.	.	R	R	.	.	A	.	R	.	.	.	.	C	R	.	.	F	.	.	.	.	.	F	.	.	.		
SBGN15	182,0	F	M/P	R	R	C	R	.	R	F	F	.	R	A	.	R	.	.	R	.	C	F	R	F	F	R	R	R	.	.	F	.	.	.		
SBGN16	142,0	F	P/M		R	C	F	.	.	R	F	.	.	C	.	R	.	.	.	.	C	F	R	.	C	.	.	.	R	.	C	R	.	.		
SBGN16/A	125,0	F	M/P		R	C	F	.	R	F	F	.	.	C	R	R	.	.	.	.	C	F	R	R	C	.	.	R	R	.	F	.	.	.		
SBGN17	122,0	F	M/P		.	C	R	R	.	R	R	.	.	C	.	.	.	R	.	.	C	R	R	.	C	.	.	R	.	R	R	.	.	.		
SBGN19	57,0	F	P/M		R	F	R	.	R	F	R	R	.	C	.	F	.	.	.	.	A	C	R	R	R	.	.	R	.	.	F	.	.	.		

(a): **A** (abundant): >30 spec.s for view; **C** (common): 10 to 30 spec.s for view; **F** (few): 1 to 10spec.s for view; **R** (rare): 0.1- 1 spec.s for view; **P** (presence): < 0.1spec.s for view; **B** (barren): no specimens. The abundance classes for the single species and the reworking are as follows: A (abundant): >30%; C (common): 10 to 30%; F (few): 1 to 10%; R (rare): 0.1-1 %; P (presence): < 0.1%.

(b)**: G** (good): little or no evidence of dissolution and/or secondary overgrowth; fully preserved diagnostic characters. **M** (moderate): dissolution and/or secondary overgrowth; partially altered primary morphological characteristics; nearly all specimens can be identified at the species level. **P** (poor): severe dissolution, fragmentation and/or secondary overgrowth; largely destroyed primary features; many specimens cannot be identified at the species and/or at generic level.